Ferroelectrics

ISSN: 0015-0193 (Print) 1563-5112 (Online) Journal homepage: http://www.tandfonline.com/loi/gfer20

Focusing efficiency evaluation of ultrasonic energy for fabricated Fresnel lens through surface profile estimation and FEA

Tuan-Anh Bui & Min-Chun Pan

To cite this article: Tuan-Anh Bui & Min-Chun Pan (2017) Focusing efficiency evaluation of ultrasonic energy for fabricated Fresnel lens through surface profile estimation and FEA, Ferroelectrics, 506:1, 76-92, DOI: 10.1080/00150193.2017.1282258

To link to this article: http://dx.doi.org/10.1080/00150193.2017.1282258

Published online: 20 Mar 2017.

FERROELECTRICS
2017, VOL. 506, 76–92
http://dx.doi.org/10.1080/00150193.2017.1282258

Taylor & Francis
Taylor & Francis Group

Focusing efficiency evaluation of ultrasonic energy for fabricated Fresnel lens through surface profile estimation and FEA

Tuan-Anh Bui[a] and Min-Chun Pan[b]

[a]School of Mechanical Engineering, Hanoi University of Science and Technology, Hanoi, Vietnam; [b]Graduate Institute of Biomedical Engineering and Department of Mechanical Engineering, National Central University, Jhongli City, Taoyuan County, Taiwan, R.O.C

ABSTRACT

High focusing efficiency of a multi-level Fresnel lens is desired when it is designed and fabricated. How to estimate the focusing efficiency is an important issue after the Fresnel lens is made. We propose a method to evaluate the focusing efficiency of the fabricated Fresnel lens based on its surface profile. The profile of Fresnel lens fabricated shows how similar to the designed, which has been theoretically predicted a maximal focusing efficiency such as 81% and 40.5% for a four-phase and two-phase level Fresnel lenses, respectively. This method can be applied to evaluate the focusing efficiency of any fabricated surface profile of Fresnel lenses prior to a direct experimental measurement for energy focusing. The focusing efficiency of a four-phase level Fresnel lens designed to operate at a frequency of 100 MHz of an ultrasonic ejector, which was fabricated by a two-mask process using SU-8 photoresist, approximate 60% is illustrated. Finite element analysis was employed to confirm and observe the energy focusing phenomenon of ultrasonic ejector models.

ARTICLE HISTORY
Received 2 March 2016
Accepted 23 November 2016

KEYWORDS
Fresnel lens; energy focusing efficiency; FEA

1. Introduction

Ultrasonic focusing lens takes charge of focusing ultrasound generated by a piezoelectric transducer for the purpose of droplet ejection in a printing device. Recently, various types of ultrasonic focusing lens have been investigated and fabricated such as spherical lens, reflection wall [1–3], Fresnel lens [4–7], self-focusing acoustic-wave liquid ejector [8], and a new type of lens using air as acoustic reflector which required no tight thickness control for effective focusing [9], etc. Fresnel lenses offer advantages of planar geometry and relative ease of fabrication over other forms of the lenses. However, the geometry is critical for efficient energy focusing, and thus tight control of the thickness of lens elements is usually required. The design and fabrication of "binary" acoustic Fresnel lenses which use multiple-phase levels to approximate the curvature of a spherical focusing field offer high efficiencies, were proposed and carried out.

CONTACT Tuan-Anh Bui anh.buituan@hust.edu.vn

Color versions of one or more of the figures in the article can be found online at www.tandfonline.com/gfer.

Hadimioglu et al. [5] presented the fabrication of two- and four-phase level Fresnel lenses with an operation frequency of 1 and 170 MHz, and illustrated the measurement of focusing efficiency. They showed that focusing efficiencies of 170 MHz two- and four-phase level Fresnel lenses are close to the theoretical values, which are about 40 and 80%, respectively. Meanwhile, the focusing efficiency of 1 MHz 4 phase Fresnel lens exhibits significantly superior to the 2 phase lens, as it achieves the theoretically predicted value of 80%. Chan et al. [10] proposed performing finite element analysis for evaluating energy distribution of multilevel acoustic Fresnel lens. They indicated that a high focusing efficiency about 81% was obtained for the Fresnel lens with a number of phase levels larger than four. Levy et al. [11] reported an efficiency analysis of diffractive optical lenses, and proposed the efficiency to be evaluated by a weighting sum of the contributions from each region of the lens.

To improve the focusing efficiency of ultrasound energy, in the previous study [12] we developed some methods to fabrication the Fresnel lens, such as two-mask, three-mask process with/without SiO_2 hard mask, using positive/negative photoresist (PR). In order to estimate the energy focusing efficiency of the fabricated lenses prior to actual test, here, we employ measured surface profile of a four-level Fresnel lens with operating frequency of 100 MHz, which was fabricated by a two-mask process using SU-8 PR, to approximately evaluate its focusing efficiency. To justify the proposed method the finite element analysis (FEA) is applied to verify the result obtained by the evaluation. An agreement between estimation and numerical simulation was achieved so that the proposed method can be considered as a tool to evaluate the focusing efficiency and compare various fabrication processes of multi-phase level Fresnel lenses.

2. Estimation of focusing efficiency of fabricated Fresnel lens

A. Fabrication of Fresnel lens

For the purpose of focusing ultrasound at the focal plane of the lens, the design parameters of Fresnel lens are related to the phase level number, working frequency, and sound velocity in the coupling medium and the lens substrate. In this study, a 100 MHz four-phase level Fresnel lens was designed and manufactured from silicon wafer. Therefore, the step height and maximal radial distance of the lens are $h = 4.55$ and $r_{max} = 244$ μm, respectively [12]. With the designated parameters the focusing lens includes four regions, in which a four-phase level exists in each region, as shown in Fig. 1.

In our previous study [12], we developed a feasible fabrication of Fresnel lens using two masks associated with two etching steps. A two-mask fabrication process employing SU-8 in the lithography was applied to address the difficulty of non-uniform photoresist coverage because of the high aspect ratio (ratio of the feature height to its width) of the lens. The fabrication processes of acoustic focusing lens were carried out by two cycles corresponding to two different masks. In the first cycle fabrication, the Si substrate was etched with the depth of $2h$ (h: the step height of Fresnel lens). And then, the wafer was aligned and exposed with using the 2nd mask and repeated the same processes with the depth of Si etching h in the second cycle. Figure 2 briefly illustrates the process of fabricating the designated Fresnel lens.

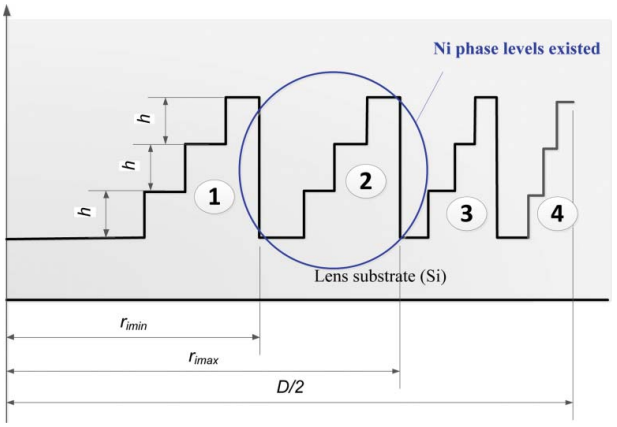

Figure 1. Designated profile of Fresnel lens; h denotes step height; D is the diameter of Fresnel lens.

B. Focusing efficiency estimation for fabricated Fresnel lens

High focusing efficiency of a Fresnel lens is desired although this depends on its actual fabrication. This study presents an estimation method for energy-focusing efficiency employing measured surface profile data. In general, focusing efficiency of an N-phase-level Fresnel lens, which is also called the first-order diffraction efficiency, can be theoretically estimated by

$$\eta_N = \left[\frac{\sin(\pi / N)}{\pi / N}\right]^2. \tag{1}$$

This equation is used to predict the ideal value of the efficiency. However several factors affecting the actual performance must be considered in the evaluation because they may lead

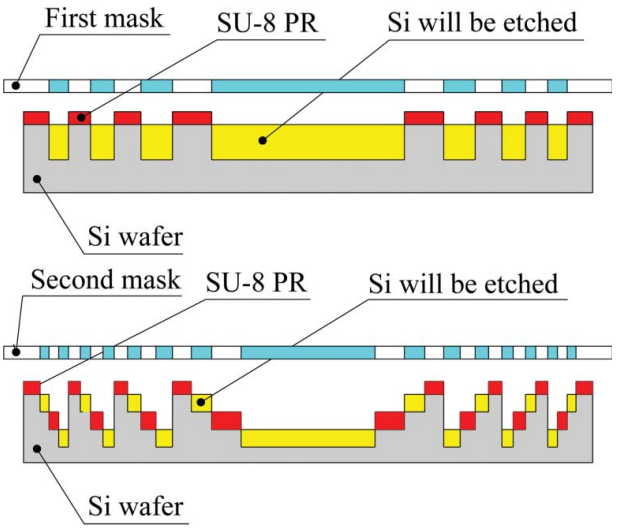

Figure 2. Illustration of a two-mask fabrication process for a 4-phase level Fresnel lens.

to lower total efficiency. Particularly, fabrication errors may contribute to major efficiency reduction; besides, the loss of acoustic energy transmitting through the lens and the printing medium also results in lower overall efficiency.

The total efficiency can be considered as a weighted sum of partial efficiencies of each region constructing the lens because the number of phase levels existing in these regions may differ from the design. If only the influence of lateral dimension of surface profile is taken into account, the efficiency can be evaluated as [11]

$$\overline{\eta} = \sum_{N_i} \gamma_{N_i} . \eta_{N_i}, \tag{2}$$

where γ_{N_i} and η_{N_i} are the weighting coefficient and (as before) the focusing efficiency of a region, respectively, for an existing N_i phase level.

For plane-wave transmission through the lens, assume the contribution of each region N_i phase levels given by the relative area of the lens. Then, the weighting coefficient can be evaluated by [11]

$$\gamma_i = \int_{r_{\text{imin}}}^{r_{\text{imax}}} rdr \Big/ \int_0^{D/2} rdr = \frac{4}{D^2}\left(r_{\text{imax}}^2 - r_{\text{imin}}^2\right), \tag{3}$$

where r_{imax} and r_{imin} bound the region N_i phase levels; D is diameter of the lens. Thus, the weighting coefficients corresponding to the dimension of each lens region are listed in Table 1. The fabrication errors may vary the number of phase levels and degrade the profile in each region, but it is not the designated; therefore, the errors affect the actual partial focusing efficiency. By using Eq. (1), the partial efficiencies of a four-, three-, and two-phase level regions are estimated about 81%, 68%, and 40.5%, respectively.

In order to estimate the focusing efficiency more accurately, the influence of the etching depth should be considered. In the proposed estimation, the "cross-section area" of each valleys covered by the surface profile is counted by the cross-section area of the existing region N_i phase levels. Here, a new coefficient i_i called as the identity coefficient is proposed, which is defined as the ratio of cross-section area of the region of fabricated surface profile to that of the designated surface profile, i.e.,

$$i_i = \frac{A_{i-fab}}{A_{i-des}} \tag{4}$$

for the case of under etching, or

$$i_i = \frac{A_{i-des}}{A_{i-fab}} \tag{5}$$

if over etching happens during fabrication, where, $A_{i\text{-}des}$ and $A_{i\text{-}fab}$ denote the cross-section

Table 1. Parameters of Ni phase level existing regions of a Fresnel lens.

	Region 1	Region 2	Region 3	Region 4
r_{min} (μm)	0	119.40	170.10	209.8
r_{max} (μm)	119.4	170.10	209.80	244
γ_N (%)	24	25	25	26

area of the i^{th} designated and fabricated regions, respectively. Thus, the overall efficiency can be revised as

$$\overline{\eta} = \sum_{N_i} i_i . \gamma_{N_i} . \eta_{N_i} \tag{6}$$

In actual fabrication, the profile of Fresnel lens may include 4-phase level in all 4 regions of the surface profile for an ideal case, or 2-, 3- or 4-phase level in the various regions. As mentioned above, the Fresnel lens was fabricated by applying a two-mask process using SU-8 PR. The surface profile of the lens was measured using SEM (Fig. 3) to evaluate the fabrication quality. Figure 4 illustrates both the designated and measured surface profile as a comparison. It is noted in Fig. 4(b) that all four levels were not formed in the outer two regions, as the etching rate in these regions is apparently smaller than the inner regions due to smaller trench widths. This phenomenon is called as the "loading effect" when a deep etching taken in regions with different widths [13]. Therefore, in the case here the fabricated lens can be considered as it has two regions with 4 not-perfect phase levels and the other two with 3 incomplete phase levels. Based on the measurement for the 'etching' cross-section area, the identity coefficients can be calculated. as listed in Table 2.

For an ideal profile of Fresnel lens containing two regions existing 4-phase level and two regions with 3- phase level, the efficiency applying Eq. (6) can approach 74.4%. To compare with the ideal efficiency, the identity and weighting coefficients of the fabricated lens are determined according to the surface profile measurement. The boundary of each region is determined by two parameters, which are r_{i_min} and $r_{i\_max.}$. Table 3 shows the actual weighting coefficients determined from experiment data. As a result, the focusing efficiency of fabricated Fresnel lens estimated by Eq. (6) is approximate 60%.This value is a bit smaller than that of the ideal profile of the case, about 74.4%, which results from the fabrication mainly and from measurement errors partly.

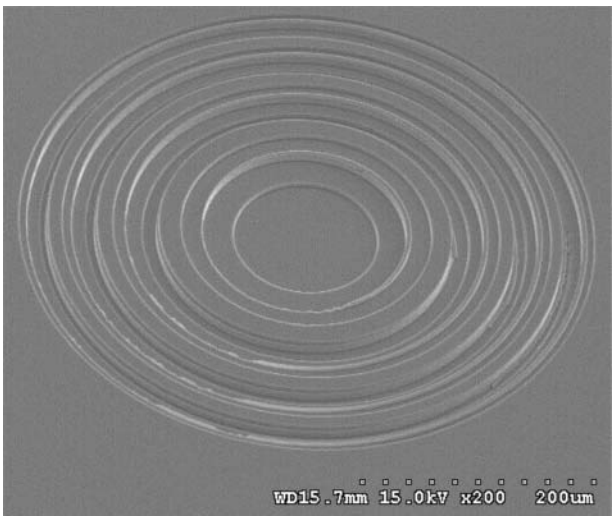

Figure 3. Fresnel lens fabricated by a two-mask process using SU-8 PR.

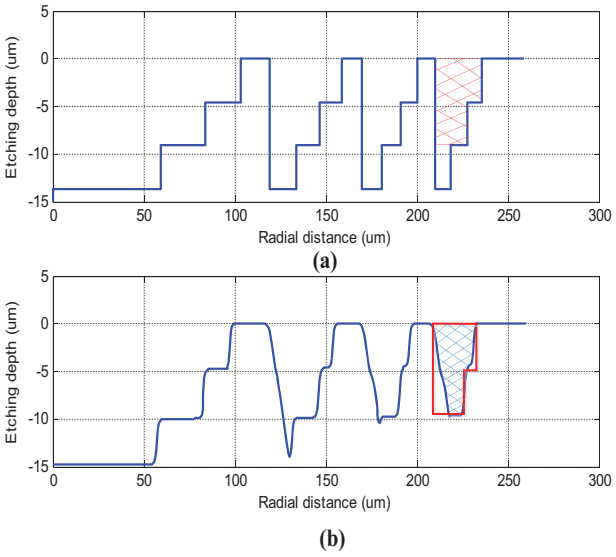

Figure 4. The profiles of (a) designated and (b) fabricated 4-phase level lens.

3. Finite element analysis for ultrasonic focusing ejectors

In the previous section, the ultrasonic focusing efficiency is evaluated by considering the influence of shaped lens surface profile. It is knows that the traditional approach in designing a multilevel Fresnel lens is typically based on the scalar theory. Moreover, the focusing characteristic analysis is limited by the assumptions of the scalar theory. The dimensions of the surface relief structure are five times smaller than the relevant wavelength. Thus, it is not satisfied in the case of high frequency applications [10].

Finite element analysis has been widely applied in solving the problems in modern industrial application. The analysis of acoustic problems using the FEA is a popular practice in many engineering processes. In the study, the ultrasound energy focusing formulation of an ejector is analyzed through FEA to verify the proposed estimation. The commercial software package COMSOL is employed to simulate the ultrasound waves transmitting through

Table 2. Cross-section areas of designated and fabricated profile of Fresnel lens.

	Region 1	Region 2	Region 3	Region 4
Designated Area (μm^2)	1123	369.14	232.91*	198.48*
Fabricated Area (μm^2)	1170	281.9	182.7	147.15
Identity coefficient i_i (%)	96	76.37	78.45	74.14

*area calculated for a complete 3-phase level.

Table 3. Actual Weighting coefficient of each region of fabricated lens.

	Region 1	Region 2	Region 3	Region 4
r_{i_min} (μm)	0	116.47	169.01	207.72
r_{i_max} (μm)	116.47	169.01	207.72	243.46
Actual Weighting Coefficient γ_N (%)	22.78	25.19	24.49	27.08

Fresnel lens and ejecting liquid to estimate the energy focusing efficiency. The analysis is conducted not only in analyzing a spherical lens and an ideal four-level Fresnel lens, but in evaluating the efficiency of the fabricated lens that was presented in the previous sections.

A. Finite element formulation

The basic theory of acoustic waves here is based on some assumptions. To simplify the Navier-Stokes equation to Euler equation, viscosity and thermal conductivity are neglected in the beginning of an acoustic process [14]. The conversion of mass is described by a following partial differential equation.

$$\rho_0 \frac{\partial u}{\partial t} = -\nabla p \tag{7}$$

Since the theory of linear acoustic, when the density varies with position, we have

$$\frac{\partial^2 p}{\partial t^2} = \rho c^2 \nabla . \left(\frac{1}{\rho} \nabla p \right) \tag{8}$$

On the contrary, when density is independent on position, Eq. (8) becomes

$$\frac{\partial^2 p}{\partial t^2} = c^2 \nabla^2 p \, . \tag{9}$$

Equation (9) is said to be the linear wave equation for sound propagation in liquid with a sound speed *c*. It is noted that in case of time-harmonic wave the pressure varies with time, and it can be described as

$$p(x, y, z, t) = p(x, y, z) e^{i\omega t} \, , \tag{10}$$

where $\omega = 2\pi f$ is called the angular frequency, and f denotes the periodic frequency. For a 2D axisymmetric geometry, the wave equation becomes [14]

$$\frac{\partial}{\partial r} \left(-\frac{r}{\rho} \frac{\partial p}{\partial r} \right) + r \frac{\partial}{\partial r} \left(-\frac{1}{\rho} \frac{\partial p}{\partial z} \right) - \left[\left(\frac{\omega}{c} \right)^2 - \left(\frac{m}{r} \right)^2 \right] \frac{rp}{\rho} = 0 \, , \tag{11}$$

where m is the circumferential wave number; r and z are the two independent variables corresponding to the radial and axial coordinates. When solving the wave equation, it will be constrained by the boundary conditions, which will be specifically determined for each problem. The elastic wave propagation with a short wavelength can be analyzed by solving the structural dynamic equation [15]

$$[M]\{\ddot{U}\} + [C]\{\dot{U}\} + [K]\{U\} = \{F(t)\} \tag{12}$$

where [M], [K], [C] denote the mass, stiffness and proportional damping matrices; {F}is the external load vector; $\{U\}, \{\dot{U}\}, and \{\ddot{U}\}$ are the nodal displacement, velocity and

acceleration vectors of the structure. Notice that when discretizing the model, the time and space steps would be limited and they can be estimated by means of the inequality

$$\Delta t < \Delta x / v\,, \tag{13}$$

where Δt and Δx are the discretization steps in time and space, respectively, and v is the wave velocity in the media. Choosing an adequate integration time step, Δt, can obtain the accuracy of the solution. The smaller integration time steps are, the better accuracy of the model is obtained, but it takes longer computation time. Therefore, a compromise is expected, and a rule of thumb employs 20 points per cycle of the highest frequency, i.e. [16]

$$\Delta t = \frac{1}{20 f_{\max}}\,. \tag{14}$$

The space step is chosen as a recommendation that the wavelength in the domain contains 10 to 20 nodes [16]. In this study, the purpose is to see the ultrasonic energy focusing phenomenon, and to save time in computing the model, the triangular shaped elements were meshed with a reasonable element size, which contains about 10 nodes per a wavelength.

B. Numerical simulation for a spherical lens

Spherical surface is an ideal geometry of a focusing lens that is expected to obtain the highest energy focusing efficiency. In this section, we build a model employing a concave surface with the same diameter as the designated Fresnel lens. This FEA simulation aims to justify the focusing efficiency estimation before. A half section plane, as shown in Fig. 5, is employed for the finite element modeling due to the axis- symmetrical geometry. The boundary conditions employed in the analysis include (1) plane wave, which is assumed as the output signal of a piezoelectric transducer and input signal from the bottom boundary of the models; (2) axial symmetry at $r = 0$; and impedance boundary condition is applied at the borders (3), (4) and (5) of the models, which is constrained by an expression as follows

$$n \cdot (-\nabla p) = \frac{i\omega p}{Z}\,, \tag{15}$$

where Z is the acoustic impedance.

The lens substrate in the model is made of silicon with the longitudinal sound wave velocity $v_l = 6880$ m/s, and the density $\rho = 2330$ kg/m^3. In the simulation, water is selected as the coupling medium, already contained in the material library of COMSOL. Sound wave velocity in water with density $\rho = 1000$ kg/m^3 is given by $v_m = 1500$ m/s. Besides, the FEA model is simulated with a frequency of $f = 100$ MHz; this information is used to determine the mesh size as discussed above. The spherical lens is modeled with a 550 μm thick of silicon wafer. The maximum element size is about 1.5 μm and 6.8 μm in water and lens regions, respectively. Figure 6 illustrates part of the finite element modeling with nodes and elements near the lens profile.

Generally the ultrasonic wave travels in a lens faster than in the surrounding medium, concave ultrasound lenses are focusing. And, the ultrasound energy is expected converging toward a focal point. For a plano-concave lens with a radius of curvature R attached to a

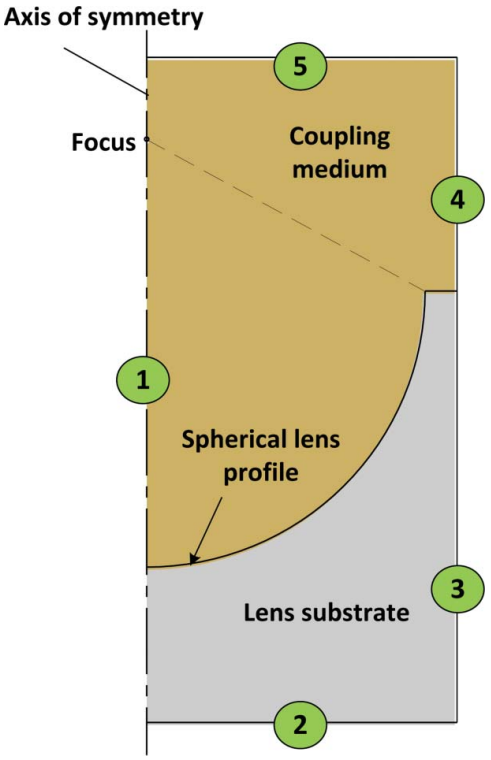

Figure 5. Half cross-section for the axis-symmetrical geometry of a spherical lens.

piezoelectric transducer surface, the focal length z_0 is estimated by

$$z_0 = \frac{R}{1 - c_M / c_L}, \tag{16}$$

where c_M and c_L are the velocities of ultrasound in the medium and lens, respectively.

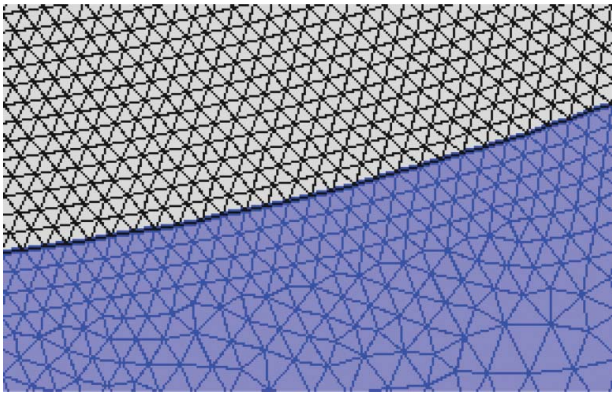

Figure 6. Mesh size and distribution near spherical lens.

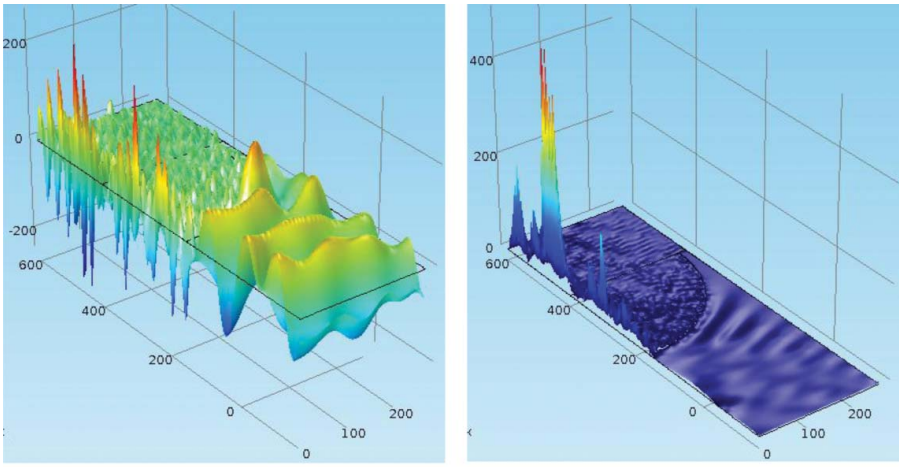

Figure 7. Computed acoustic (a) pressure and (b) intensity field for the spherical lens.

The acoustic pressure and intensity fields in the half plane are characterized in Fig. 7. The pressure is apparently high along the symmetrical axis with an expectation of high intensity in the axis. It is noted that the acoustic intensity concentrates on some regions along the axis. The dominant peak is, however, at a zone slightly lower than the expected height of the focal point. This mismatch position of the focal regions probably results from the ultrasound velocity (1500 m/s) used to compute the focal length in Eq. (16) different from that used in FEA with a default value of COMSOL.

The focusing efficiency of acoustic energy can be evaluated by the ratio of the full width half maximum (FWHM) energy of the focal region to the total energy in the focal plane. Figure 8 shows the energy distribution along the cross-section slice of the focal plane of the ideal spherical structure. Therefore, the focusing efficiency of the spherical lens obtained from simulation is about 84.6%. Obviously, it is not as high as the theoretical focusing efficiency (100%) obtained from optical theory. It is noted that ultrasonic wave was used in the simulation, which is different from monochromatic source used in optical theory; and it is

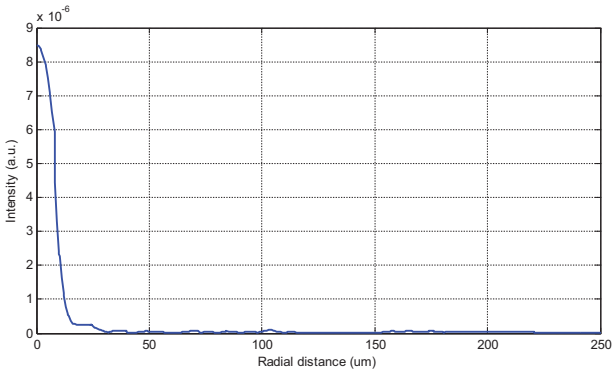

Figure 8. Intensity distribution in the focal plane for the model of spherical lens.

probably the main reason causing the difference besides the errors of numerical computation. Nevertheless, the FEA can still be used as a tool to estimate the focusing efficiency for any fabricated Fresnel lenses.

C. Numerical simulation of the designated and fabricated lens

Two FEA models were built up to simulate the ultrasound energy focusing for a comparison. The first model with an ideal profile was expected to see a high focusing efficiency in simulation, and the second with an actual fabricated profile was also performed numerical analysis to justify the result of proposed evaluation.

Based on the axisymmetric nature of the model, a two- dimensional model was made in order to save computation time. In the model, the Fresnel lens is modeled at the surface of a 550 μm-thick Si wafer, and this surface contacts with the coupling medium. Because of the axisymmetric property, the focal point of the lens is along the symmetrical axis of the device. The four-level Fresnel lens designed with a lens thickness about 15 μm and its diameter of 488 μm, the focal length, which is designed with F-number of unit, is about 488 μm, and is immersed in the coupling medium. Figure 9 illustrates the geometric profiles used in the simulation. Parts of the finite element modeling with nodes and elements near the lens profile are illustrated in Fig. 10. The simulation was performed with all the parameters same as the above spherical model. Likewise, the boundary conditions including plane wave, axial symmetry at $r = 0$, and impedance boundary condition were also applied in these two models.

The acoustic wave propagation through the structure was computed in the simulation. Hence, the acoustic energy in the form of planar wave transmits through the Fresnel lens

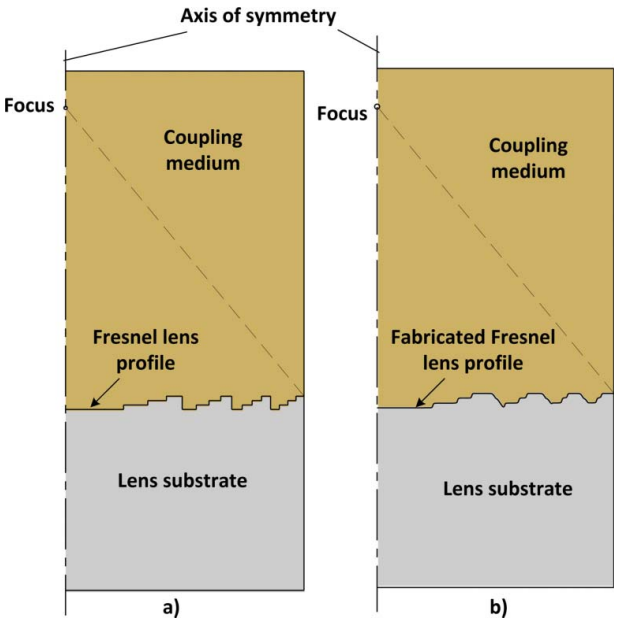

Figure 9. Half cross-section for the axis-symmetrical geometry of (a) designated and (b) fabricated Fresnel lens.

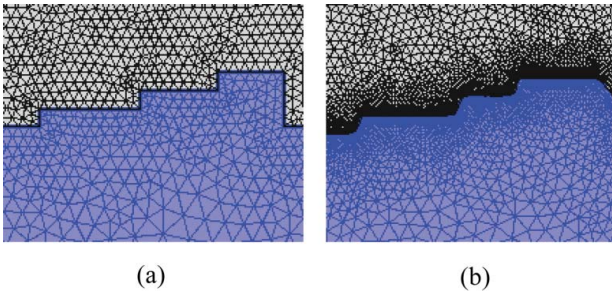

Figure 10. Illustration of mesh size and distribution for (a) designated and (b) fabricated Fresnel lens.

and then the coupling medium, and expected to build up around the focal zone. That means the phase-shifted plane wave interferes constructively as the acoustic wave propagates along the coupling medium.

Figure 11 shows computed acoustic pressure fields in the two structures. We can see a high acoustic-pressure distribution around the focal zone. The energy focusing phenomenon occurs at this region. Besides, the acoustic intensities of the two models, as illustrated in Fig. 12, show that most acoustic energy transmitting through the structures converges around the focal zone. It confirms the constructive interference of phase-shifted plane waves

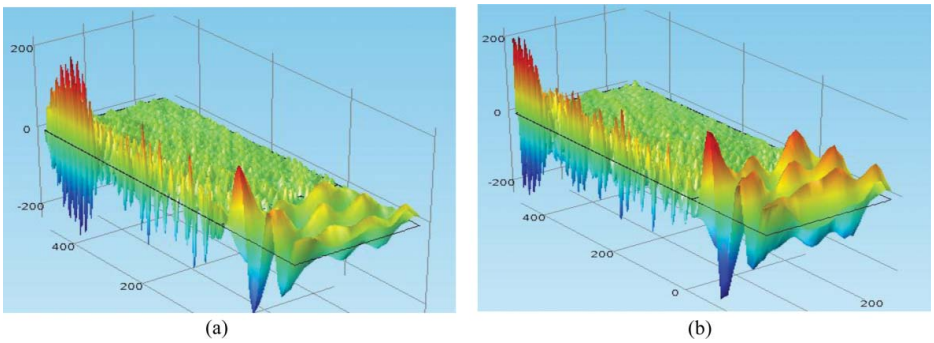

Figure 11. Computed acoustic pressure field for (a) designated and (b) fabricated Fresnel lens.

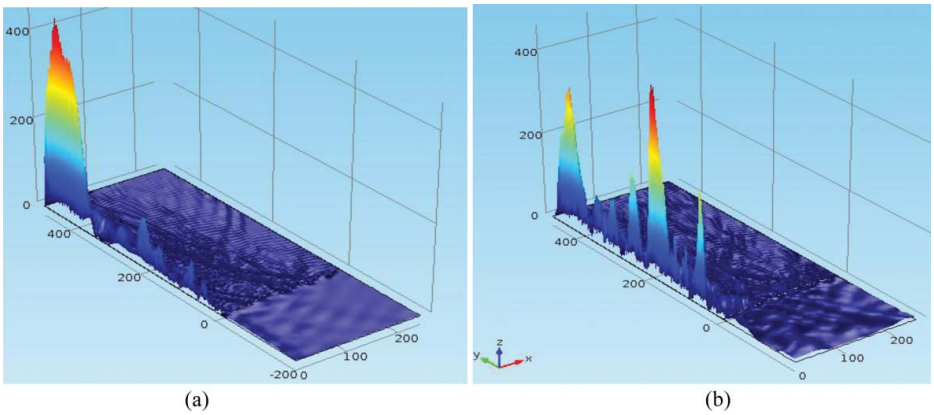

Figure 12. Computed acoustic intensity field for (a) designated and (b) fabricated Fresnel lens.

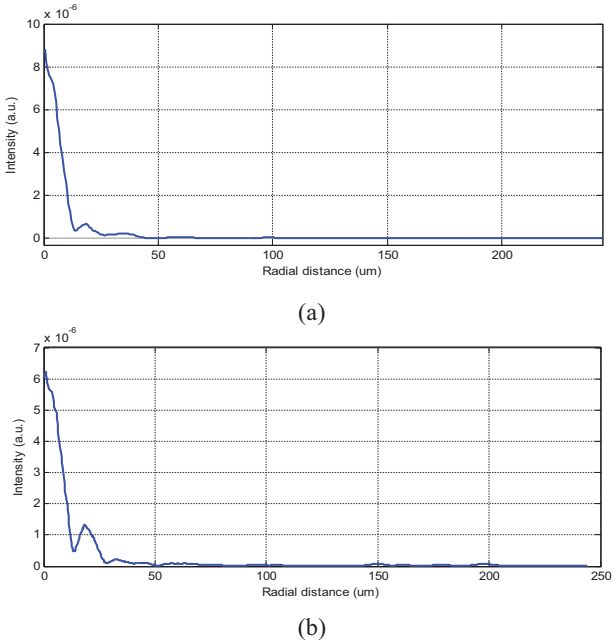

Figure 13. Intensity distribution in the focal plane for (a) designated and (b) fabricated Fresnel lens.

in the coupling medium when the acoustic waves travel through. For the case of fabricated lens the acoustic energy is, however, not all focused in the focal area although it distributes on the axis of symmetry of the structure, as shown in Fig. 12(b). The reason is that the actual profile of fabricated Fresnel lens differs from that of the designed (ideal profile); therefore, the acoustic wave reaching the surface profile of the lens diffracts in different directions and goes forward to various focal areas along the symmetry axis.

Figure 13 shows the intensity distribution along the cross-section slice of the focal planes of the designated and fabricated structures, respectively. The energy focusing efficiencies, which were estimated by the FEA for the models of designated and fabricated profiles and through the theoretical prediction (Eq. (1)) for a 4-level Fresnel lens, are shown in Table 4 for comparison. The efficiency of the ideal Fresnel lens is approximate 75%, worse than that obtained by the scalar theory, about 81% for a 4-level Fresnel lens. This disagreement results from the source radiation which is assumed monochromatic in the scalar theory; meanwhile in the FEA, we used plane wave radiation with a finite bandwidth so as to result in an acoustic dispersion. Besides, the simulation results are influenced by the input material properties and assumed boundary conditions used in the computation. It is noted that the efficiency of the fabricated Fresnel lens is much smaller than that of the ideal lens. Actually, the imperfect fabricated lens profile degrades convergence of ultrasonic wave to a focal zone. It may cause

Table 4. Energy focusing efficiency evaluated by FEA and theoretic prediction.

	FEA for ideal 4-level Fresnel lens	FEA for fabricated 4-level Fresnel lens	Theoretical prediction for 4-level Fresnel lens (Eq. (1))
Focusing efficiency	0.75	0.63	0.81

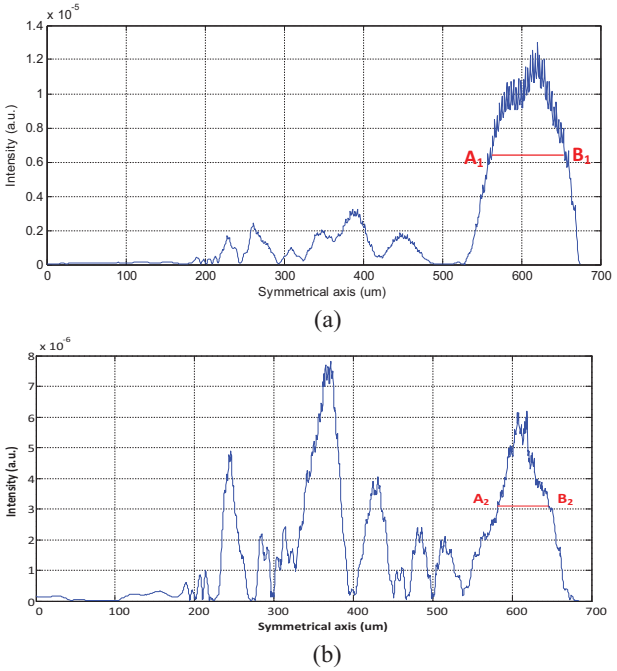

Figure 14. Intensity distribution along symmetrical axis for (a) designated and (b) fabricated lens.

the phenomena of diffraction and refraction at the same time when the ultrasound reaches the surface profile after traveling through the acoustic lens. Therefore, some acoustic dispersion at the surface profile and some interference zones along the axis of symmetry are created. Although the majority of acoustic energy was driven to the focal zone, however, other interference zones also occupied a part of the energy in those regions. That means the energy focusing efficiency will be lower than the expectation, which is 75% in the simulation. Additionally, as mentioned before the efficiency estimated by the proposed evaluation is about 60% for the fabricated Fresnel lens. This value is slightly smaller than the simulation result. To a certain extent we have obtained a reasonable agreement between these two results.

The focusing efficiency of Fresnel lens was estimated by the ratio of FWHM energy to total energy at focal plane. Furthermore, since the formation of liquid droplets is generated by the energy around focal region. Thus, it is reasonable to estimate the efficiency of generating a droplet. Figure 14 shows the intensity distribution in the symmetrical plane for both designated and fabricated lens models. Assuming that the energy in the FWHM of intensity distribution around the focus (between A_1 and B_1, A_2 and B_2 in Fig. 14) dominates the droplet formation; it is significant to estimate the energy in various planes around the FWHM of focus region. Figure 15 presents the intensity distribution in those planes. The high intensity is observed around the central area of HWHM, and gradually reduces to two sides; it means that most of energy is taken in estimation of the efficiency. To simplify the estimation of total energy around the focal region, we assume that the energy is constant between two adjacent examined planes. Thus, we can calculate the total energy in volume for the region. The overall focusing energy is considered as a ratio of total FWHM energy to total energy in volume; therefore, it is about 72% and 63% for the designated and fabricated lens models, respectively. It is noted that these efficiencies are rather closed to the values estimated in the

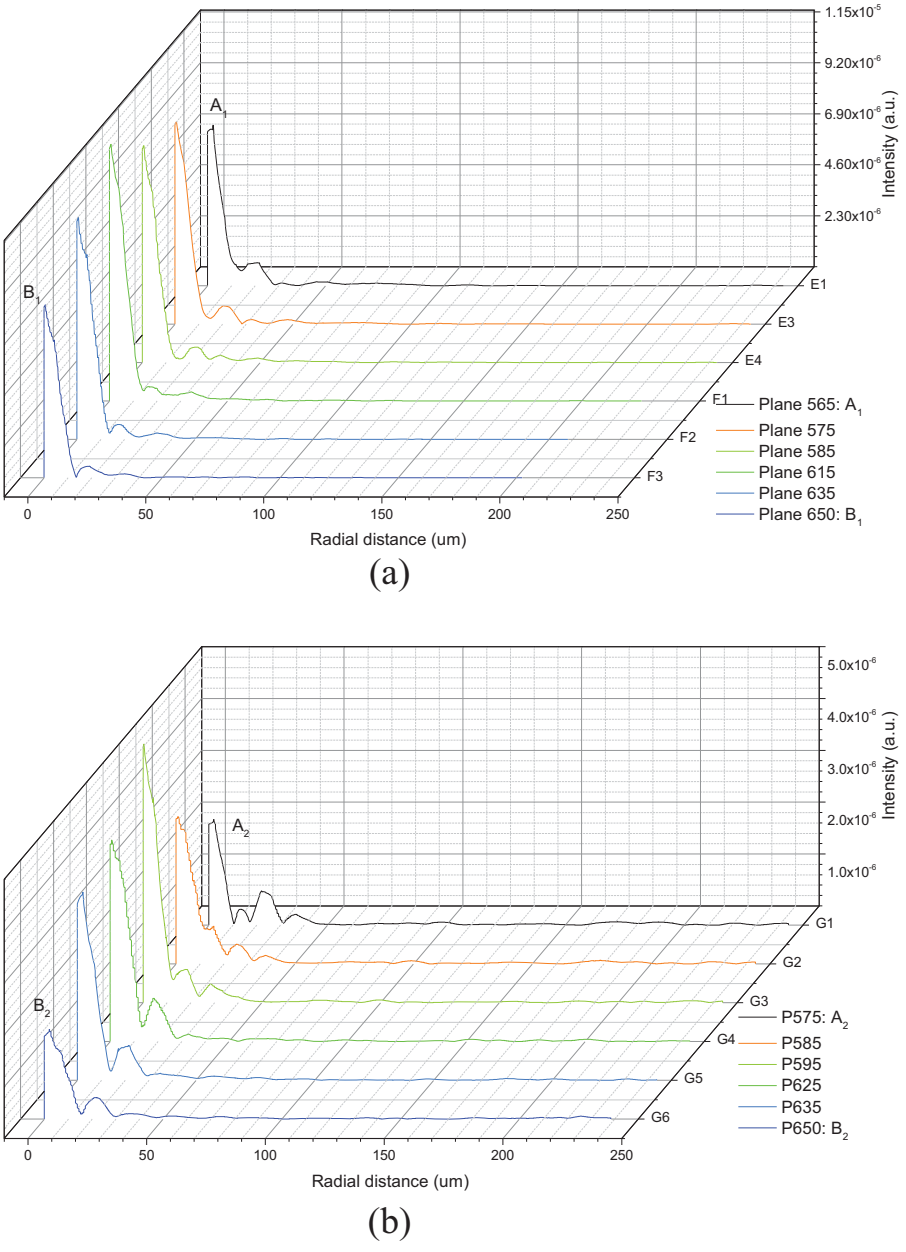

Figure 15. Intensity distributions of various planes along symmetrical axis for (a) designated and (b) fabrication lens.

focal plane, which are 75% and 63% for the designated and fabricated models, respectively. The simulation result confirms that most of the energy is focused around the focal region. And, the efficiencies estimated by using energy in the focal plane and focal region in volume are not much different. It is really significant for tried fabrication to roughly estimate the efficiency of a surface profile of a fabricated Fresnel lens that the energy calculation in a plane is much easier than in a region.

The study illustrates the proposed and implemented method being a useful tool for a rough estimation of energy focusing efficiency although the simulation result cannot exactly characterize the performance of an actual device. Especially in the trailed fabrications, one can employ such an estimation to find a reasonable profile of the Fresnel lens instead of proceeding with a complicated fabrication process to obtain only slightly higher efficiency.

4. Conclusions

The achievable energy focusing efficiency of a fabricated four-phase level Fresnel lens has been evaluated through using the measured lens profile, i.e., to estimate the focusing efficiency of a 100 MHz four-phase level Fresnel lens of an ultrasonic ejector. In the study the lens was fabricated through a two-mask process employing SU-8 PR, and achieved about 60% efficiency. The estimation investigates the influence of geometry of a multilevel Fresnel lens on its focusing efficiency, in which the ideal efficiency is calculated based on the scale theory for optics. Furthermore, the FEA was used to verify the efficiency obtained by the proposed estimation. The study shows the FEA is able to approximately estimate the focusing efficiency in the trailed fabrications of the Fresnel lenses. An agreement between the numerical simulation and proposed estimation was presented.

References

1. S. Kameyama, H. Fukumoto, T. Kimura, S. Wadaka, Ink Mist Jet Generation Using Low Frequency Focused Ultrasonic Waves and Nozzle. *1999 IEEE Ultrasonics Symposium*, 695–698 (1999).
2. H. Fukumoto, J. Aizawa, H. Matsuo, H. Narumiya, K. Nakagawa, Liquid Ejector Which Uses a High-Order Ultrasonic Waves to Eject Ink Droplets and Printing Apparatus Using Same. (2000).
3. J. Aizawa, H. Fukumoto, M. Takeda, *Liquid Ejector* (2003).
4. B. Hadimioglu, S. A. Elrod, D. L. Steinmetz, M. Lim, J. C. Zesch, B. T. Khuri-Yakub, E. G. Rawson, C. F. Quate, Acoustic Ink Printing. *1992 Ultrasonics Symposium*, 929–935 (1992).
5. B. Hadimioglu, E. G. Rawson, R. Lujan, M. Lim, J. C. Zesch, B. T. Khuri-Yakub, C. F. Quate, High-Efficiency Fresnel Acoustic Lenses. *1993 Ultraoniscs Symposium*, 579–582 (1993).
6. B. Hadimioglu, S. Elrod, R. Sprague, Acoustic Ink Printing: an Application of Ultrasonics for Photographic Quality Printing at High Speed. *2001 IEEE Ultrasonics Symposium*, 627–635 (2001).
7. C. F. Quate, E. G. Rawson, B. Hadimioglu, Muti-Discrete-Phase Fresnel Acoustic Lenses and Their Application to Acoustic Ink Printing. (1991).
8. D. Huang, E. S. Kim, Micromachined Acoustic-Wave Liquid Ejector. *J. Microelectromech. Syst.*, **10** (3), 442–449 (2001).
9. C-Y. Lee, H. Yu, E. S. Kim, Acoustic Ejector with Novel Lens Employing Air-Reflectors, in Editor (Ed.)^(Eds.): *Book Acoustic Ejector with Novel Lens Employing Air-Reflectors* (edn.), 170–173 (2006).
10. S. C. Chan, M. Mina, S. S. Udpa, L. Udpa, W. Lord, Finite Element Analvsis of Multilevel Acousttc Fresnel Lenses, IEEE Trans. *Ultrason. Ferroelectr. Freq. Control*, **43**(4), 670–677 (1996).
11. U. Levy, D. Mendlovic, E. Marom, Efficiency analysis of diffractive lenses. *J. Opt. Soc. Am. A*, **18** (1), 86–93 (2001).
12. M-C. Pan, T.-A. Bui, Y.-C. Nien, W.-C. Shih, Design and Fabrication of Fresnel Lens and ZnO Thin-Film Transducer. *Jpn. J. Appl. Phys.*, **50**(7), 07HD02 (2011).
13. H. Xiao, *Introduction to Semiconductor Manufacturing Technology* (Prentice Hall, New Jersey, (2001). 2001.

14. T. Strek, Finite Element Modelling of Sound Transmission Loss in Reflective Pipe in Moratal, D. (Ed.): *Finite Element Analysis* (InTech, (2010).
15. R. Barauskas, V. Daniulaitis, Simulation of ultrasonic wave propagation in solids. *ULTRAGARSAS* **37**(4), 34–39 (2000).
16. F. Moser, L. J. Jacobs, J. Qu, Modeling elastic wave propagation in waveguides with the finite element method. *NDT and E Int.*, **32**(4), 225–234 (1999).